

Redox Instability of Copper(II) Complexes of a Triazine-Based PNP Pincer

Gholamhossein Mohammadnezhad,^{*,[a]} Ali Mohammad Amirian,^[a, b] Helmar Görls,^[c] Winfried Plass,^[c] Aaron Sandleben,^[d] Sascha Schäfer,^[d] and Axel Klein^{*,[b, d]}

Dedicated to Prof. Dr. Wolfgang Kaim on the occasion of his 70th birthday

The new Cu(I) complex [Cu(PNP^{NTPH}-Ph)Cl] (1) containing the tridentate PNP pincer ligand *N,N'*-bis(diphenylphosphino)-2,6-diamino-4-phenyl-1,3,5-triazine was obtained from the reaction of [Cu(SMe₂)Cl]_n with the ligand as ether solvate 10.5Et₂O. 1 was independently obtained from a reaction mixture containing the ligand and the Cu(II) precursor CuCl₂·2H₂O in 50% yield alongside with the Cu(II) coordination polymer [Cu(O₂PPh₂)₂]_n (2). From the reaction of Cu(NO₃)₂·3H₂O with PNP^{NTPH}-Ph in the presence of pyridine the complexes [Cu(O₂PPh₂)₂(Py)₂(H₂O)] (3), [Cu(O₂PPh₂)(Py)₂(NO₃)₂] (4), and [Cu(Py)₄(NO₃)₂]Py (5), were obtained, 2, 3, and 4 contain diphenyl-phosphinate ligands. The underlying redox reaction of the ligand and Cu(II) yielding the

oxidised ligands observed in the by-products and the Cu(I) product complex was further studied using electrochemistry and UV-vis spectroelectrochemistry. Attempts to synthesise the Cu(II) complex [Cu(PNP^{NTPH}-Ph)(NO₃)₂] (6) in a mechanochemical experiment gave evidence for this unprecedented species from ESI-MS(+) and EPR spectroscopy but also revealed its very high sensitivity to air and moisture. The catalytic activity of 1 was investigated in the azide-alkyne cycloaddition yielding various 1-benzyl-4-phenyl-1*H*-1,2,3-triazoles. The environmentally benign ("green") and cheap EtOH/H₂O solvent mixture turned out to be very suitable. Melting points, FT-IR, and NMR spectra of the triazole products were analysed.

Introduction

Transition metal complexes of the so-called pincer ligands are perfect candidates for homogeneous catalysis since they combine high complex stability with variability of their ligand scaffold permitting the tuning of their electronic and steric properties and thus reactivity and selectivity.^[1,2] This makes them very suitable for a variety of catalytic applications.^[2-7] Amongst them, pincer ligands with a PNP motive have recently

attracted attention.^[8-15] Typical ligands of this type were the well-studied *N,N'*-bis(diaryl/alkylphosphino)-2,6-diaminopyridines^[2,7-9,14-29] (PNP^{NpyR}-R', Scheme 1A), 2,6-bis((diaryl/alkylphosphino)methyl)pyridines (PNP^{CpyR}-R', Scheme 1B),^[3,5-11,14,15,30-35] the *N,N'*-bis(diaryl/alkylphosphino)-2,6-diamino-1,3,5-triazine (PNP^{NTR}-R') derivatives^[8,9,18-26,28,36-47] (Scheme 1C) and the so far unknown 2,6-bis((diaryl/alkylphosphino)methyl)-1,3,5-triazines (PNP^{CTR}-R', Scheme 1D).

Transition metal complexes with the tridentate *N,N'*-bis(PR'₂)-2,6-diamino-4-(R)-1,3,5-triazine (PNP^{NTR}-R') ligands have been reported for Ir(I) in [Ir(*PNP^{NTR}-R')(COD)] (*PNP^{NTR}-R' = singly deprotonated ligand, R = H, Me, Ph, R'-iPr, tBu, Ph, COD = 1,5-cyclooctadiene) complexes,^[35-38] in Mo(0) e.g. in [Mo(PNP^{NTR}-Ph)(CO)₃]₂,^[28] for Pd(II) in [Pd(PNP^{NTPH}-Ph)Br]Cl and [Pd(PNP^{NTPH}-Ph)Cl](CF₃SO₃)₂,^[28] for Mn(I) e.g. in [Mn(PNP^{NTR}-iPr)(CO)₂Br] (R = H, Me, Ph, NHC₃H₅),^[40-43] for Fe(II) e.g. in [Fe(PNP^{NTPH}-Ph)(MeCN)₃](BF₄)₂,^[18,19,28,43] for Co(II) in [Co(PNP^{NTR}-iPr)Cl₂] (R = H, Me, Ph, 4-CF₃-Ph),^[20-23,45] and for Ni(II) e.g. in [Ni(PNP^{NTR}-R')Cl]Cl (R = NMe₂, Me, Ph, R'-iPr, Ph).^[24,25] Most of them were used as catalysts in important transformations. E.g. the Ir(I) complexes were used in dehydrogenative alkylations,^[36] both the Mn(I) and Co(II) derivatives in borrowing hydrogen or dehydrogenative reactions,^[40,46] and the Ni(II) complexes were used in Suzuki-Miyaura coupling catalysis.^[25] Frequently, the deprotonated ligands *PNP^{NTR}-R' were reported to be important for the catalytic transformations.^[30-39,47]

Although Cu(I) and Cu(II) complexes of *N,N'*-bis(diaryl/alkylphosphino)-2,6-diamino-pyridine ligands (PNP^{NpyR}-R'; R = H; R'-iPr, tBu, Ph) were reported,^[13,17,27,29,47-49] no Cu complexes of the 1,3,5-triazine derivatives (PNP^{NTR}-R') were known to date. In a very recent report Bedford et al. describe the intrinsic

[a] Assoc. Prof. Dr. G. Mohammadnezhad, A. M. Amirian
Department of Chemistry, Isfahan University of Technology,
Isfahan, 84156-83111, Iran
E-mail: mohammadnezhad@iut.ac.ir

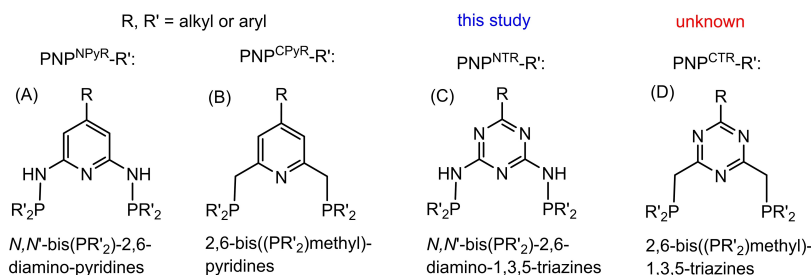
[b] A. M. Amirian, Prof. Dr. A. Klein
Chemistry Department Faculty of Science, Shiraz University,
Shiraz, 71454, Iran

[c] Dr. H. Görls, Prof. Dr. W. Plass
Lehrstuhl für Anorganische Chemie II,
Institut für Anorganische und Analytische Chemie,
Friedrich-Schiller-Universität Jena,
Humboldtstr. 8, 07743 Jena, Germany

[d] Dr. A. Sandleben, S. Schäfer, Prof. Dr. A. Klein
Department für Chemie, Institut für Anorganische Chemie,
Universität zu Köln,
Greinstraße 6, 50939 Köln, Germany
E-mail: axel.klein@uni-koeln.de
https://klein.uni-koeln.de

Supporting information for this article is available on the WWW under
https://doi.org/10.1002/ejic.202001129

© 2021 The Authors. European Journal of Inorganic Chemistry published by Wiley-VCH GmbH. This is an open access article under the terms of the Creative Commons Attribution Non-Commercial NoDerivs License, which permits use and distribution in any medium, provided the original work is properly cited, the use is non-commercial and no modifications or adaptations are made.



Scheme 1. Heteroaromatic PNP pincer ligands.

instability of the much related Cu(II) complex [Cu(PNP^{NPy}-Ph)(OAc)₂] (PNP^{NPy}-Ph = *N,N'*-bis(diphenylphosphino)-2,6-diamino-pyridine) to undergo Cu(II) reduction to Cu(I) and oxidation of the phosphine moieties in the presence of water,^[48] disagreeing with earlier claims that the Cu(II) complex is an effective catalyst in Suzuki type coupling reactions.^[47] From the same ligand a binuclear Cu(I) iodo complex has been described,^[49] while the cationic complex [Cu(PNP^{NPy}-Ph)(PPh₃)⁺] is mononuclear.^[27] For the diisopropylphosphine derivative a mononuclear Cu(I) bromido complex was reported.^[17] Very recently Cu(I) complexes with phosphalkene PNP ligands complexes with frustrated Lewis pair (FLP) type bond activation and application in catalytic CO₂ reduction was reported.^[50]

Earlier than the Bedford report,^[48] we got interested in the *N,N'*-bis(PR'₂)-2,6-diamino-4-(R)-1,3,5-triazine (PNP^{NTR}-R') ligands and the use of their Cu(II) complexes as pre-catalysts in the so-called azide-alkyne click reaction or Huisgen cycloaddition.^[51–55] A wide range of Cu(I) containing compounds has been recently developed as catalysts for this azide-alkyne 1,3-cycloaddition (AAC). However, the oxidative instability of Cu(I) species put their catalytic application in trouble. Cu(I) can oxidised or disproportionate to Cu(II) or Cu(0) and Cu(II), respectively.^[56] The most common protocols thus use Cu(II) precursors such as CuSO₄ and a reducing agent such as sodium ascorbate.^[53,54,57] The reaction of organic halides or aryl boronic acids with Na₃^[58–61] leads to the pharmacologically important 1,2,3-triazole heterocycles.^[64–67]

In this work, we describe the synthesis of the new Cu(I) complex [Cu(PNP^{NTPh}-Ph)Cl] (1) (PNP^{NTPh}-Ph = *N,N'*-bis(diphenylphosphino)-2,6-diamino-4-phenyl-1,3,5-triazine) alongside with the attempted syntheses of Cu(II) complexes with this ligand. Reaction with CuCl₂·2H₂O yielded the Cu(I) complex 1 and Cu(II) complex by-products with oxidised ligands. Reaction with Cu(NO₃)₂·3H₂O gave evidence for the Cu(II) complex [Cu(PNP^{NTPh}-Ph)(NO₃)₂] but workup yielded Cu(II) species containing diphenyl phosphinate as ligand which seems to stem from an oxidation/hydrolysis reaction sequence of the PNP ligand. The underlying redox chemistry was studied and the Cu(I) complex 1 and one of the Cu(II) complexes were successfully used as catalysts in the one-pot azide-alkyne cycloaddition reaction in the presence of water/EtOH as a green solvent.

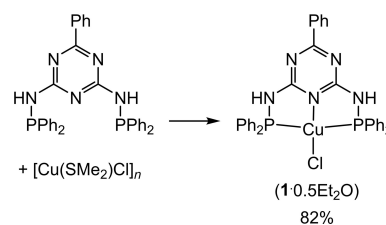
Results and Discussion

Syntheses of the PNP^{NTPh}-Ph ligand and the Cu(I) complex [Cu(PNP^{NTPh}-Ph)Cl] (1)

A modification of a previously reported procedure^[28] was used to synthesise the PNP^{NTPh}-Ph ligand. The ¹H and ³¹P NMR spectra of the ligand show an impurity of a few percent which turned out to be diphenylphosphinic acid HO₂PPh₂.

Reaction of the PNP^{NTPh}-Ph ligand with the Cu(I) precursor [Cu(SMe₂)Cl]_n in acetone solution yielded the compound [Cu(PNP^{NTPh}-Ph)Cl]·0.5Et₂O (1·0.5Et₂O) in 82% yield (Scheme 2). It contains 0.5 equivalents of co-crystallised diethyl ether as evident from NMR spectroscopy and elemental analysis.

Previously, a Cl-bridged coordination polymer [Cu(μ-Cl)(μ-κ¹-P,κ²-PN-PNP^{CPy}-tBu)]_n with a bridging κ¹-P,κ²-PN ligand was obtained from the reaction of [Cu(SMe₂)Cl]_n with the PNP^{CPy}-tBu ligand (PNP^{CPy}-tBu = 2,6-bis((di-*tert*-butylphosphaneyl)methyl)pyridine).^[15,32,33] Reaction of [Cu(SMe₂)Br]_n with the same ligand led either to the analogous polymer [Cu(μ-Br)(μ-κ¹-P,κ²-PN-PNP^{CPy}-tBu)]_n^[33] or to a mononuclear structure [Cu(κ²-PP-PNP^{CPy}-tBu)Br] with a *P,P,Br* tricoordinated Cu(I),^[34,35] which was converted to the tri-coordinated complexes [Cu(κ²-PP-PNP^{CPy}-tBu)(X)] (X=OAc^[34] or NCS^[31,35]) and also reacted to the [Cu(κ³-PNP-PNP^{CPy}-tBu)]⁺ cation with a T-shaped Cu(I) surrounding^[32–35] or the four-coordinated cations [Cu(κ³-PNP-PNP^{CPy}-tBu)(L)]⁺ (L=PMe₃ or CNtBu).^[35] Reaction of [Cu(SMe₂)Br]_n with *N,N'*-bis(diphenylphosphino)-2,6-di(methylamino)pyridine (PNP^{NPy}-Ph) allowed to crystallise the mononuclear complex [Cu(κ³-PNP^{NPy}-Ph)Br] with a tetrahedral geometry.^[29] Furthermore, a Br-bridged dimer [Cu(μ-Br)(κ²-PN-PN)]₂ with a terminal κ²-coordinating PN ligand was obtained

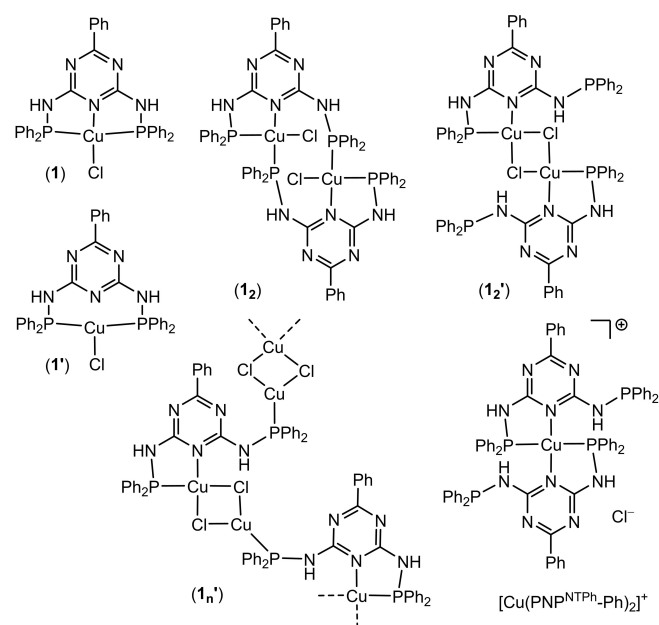


Scheme 2. Synthesis of complex 1, for possible structures of 1, see Scheme 3.

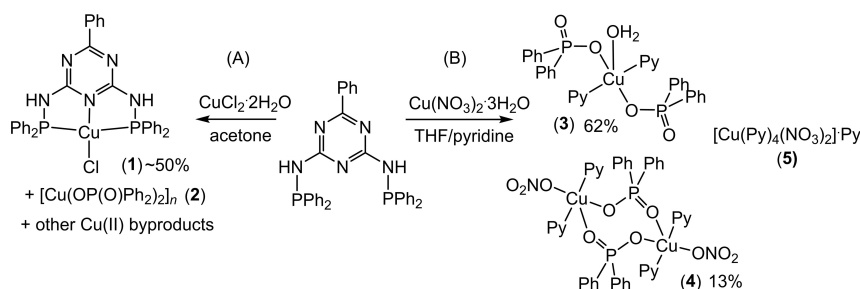
from the reaction of $[\text{Cu}(\text{SMe}_2)\text{Br}]_n$ with the PN ligand 2-((di-*tert*-butylphosphaneyl)methyl)-6-methylpyridine.^[32] Finally, the reaction of the ligand $\text{PNP}^{\text{NPy}}\text{-Ph}$ with CuI in 1:1 ratio has allowed the isolation and crystallisation of a binuclear structure $[\text{Cu}(\text{I})(\mu, \kappa^2\text{-PN-PNP}^{\text{NPy}}\text{-Ph})_2]$, with a $\kappa^2\text{-PN}$ coordinated and bridging PNP ligand. The reaction with a 2:1 ratio lead to the mononuclear complex $[\text{Cu}(\kappa^2\text{-PN-PNP}^{\text{NPy}}\text{-Ph})_2]$.^[49]

For the Ag(I) compounds $[\text{Ag}(\kappa^2\text{-PP-PNP}^{\text{CPy}}\text{-tBu)}](\text{BF}_4)$ and $[\text{Au}(\mu\text{-}\kappa^1\text{P-PNP}^{\text{CPy}}\text{-tBu})_2](\text{BF}_4)_2$ analogous $\kappa^2\text{-PP}$ or even lower $\mu\text{-}\kappa^1\text{-P}$ coordination was observed for the $\text{PNP}^{\text{CPy}}\text{-tBu}$ ligands. In contrast to this stand the Ni(II) and Pd(II) complexes with $\text{PNP}^{\text{CPy}}\text{-R}'$ or $\text{PNP}^{\text{NPy}}\text{-R}'$ ligands which all show full coordination of four ligands.^[24–26,28,68]

Therefore, the complex **1** could either adopt the assumed mononuclear structure **1** with a $\kappa^3\text{-PNP}$ coordination, the mononuclear $\kappa^2\text{-PP}$ version **1'** or the binuclear versions **1₂** or **1₂'** or the form of a coordination polymer **1n'** with a bridging $\kappa^1\text{-P}, \kappa^2\text{-PN}$ PNP ligand (Scheme 3). With a 2:1 ligand:Cu ratio the complex $[\text{Cu}(\kappa^2\text{-PN-PNP}^{\text{NTPH}}\text{-Ph})_2]^+$ with Cl^- as counter anion could possibly be formed.



Scheme 3. Possible structure of monomeric structures **1** and **1'**, the binuclear structures **1₂** and **1₂'**, the coordination polymer **1n'**, and the 2:1 (ligand:Cu) complex $[\text{Cu}(\text{PNP}^{\text{NTPH}}\text{-Ph})_2]^+$.



Scheme 4. Syntheses of complexes **1** to **5**; for possible structures of **1**, see Scheme 3.

The Cu complex **1** has limited solubility in polar organic solvents such as MeOH, EtOH, CH_3CN , DMF, and DMSO, is sparingly soluble in acetone, CH_2Cl_2 and THF and virtually insoluble in CHCl_3 , diethyl ether, or benzene. The compound is sensitive to oxygen and moisture. Solutions turn rapidly to greenish upon standing in air. The solid changed its colour to brown after exposure to air for a few days. The poor solubility is consistent with a binuclear or polymeric character in the solid state. In addition to this, dissolution in solvents with coordination potential might lead to solvent coordination at Cu(I) and further species. The FT-IR spectrum shows a strong band at 1536 cm^{-1} attributed to triazine stretching modes. The N–P vibration frequencies in the ligand were shifted from 1093 cm^{-1} to 1101 cm^{-1} upon coordination to Cu. HR-ESI-MS(+) gave unequivocal proof for the mononuclear structures **1** or **1'** showing signals for $[\text{M}]^+$ and $[\text{M}-\text{Cl}]^+$ at 653.07262 and 618.103767 m/z, respectively. However, also the binuclear structures or the polymer could give these signals in the MS experiment as masses of the dimers **1₂** and **1₂'** lie at 1306 m/z and would be probably not detectable due to spectrometer limitations. Also, complex $[\text{Cu}(\text{PNP}^{\text{NTPH}}\text{-Ph})_2]^+$ with 1173 m/z would probably not be detected. ^1H , ^{13}C , and ^{31}P NMR spectra of $10.5\text{Et}_2\text{O}$ showed broad poorly resolved signals preventing any insight into the molecular structure (Figures S1 to S6 in the Supporting Information, SI). Probably these poor spectra are due to traces of paramagnetic Cu(II) species. Regardless of the molecular structure in the solid, in fluid solution we assume monomeric species with the composition $[\text{Cu}(\text{PNP}^{\text{NTPH}}\text{-Ph})\text{Cl}]$ and will refer later to this as complex **1**.

Reactions of the $\text{PNP}^{\text{NTPH}}\text{-Ph}$ ligand with Cu(II) precursors

Reaction of the ligand with the Cu(II) precursor $\text{CuCl}_2 \cdot 2\text{H}_2\text{O}$ in acetone solution gave a dark green solution from which yellow material precipitated. From the supernatant green acetone solution no defined compounds could be isolated but Cu(II) species were assumed from the colour. Re-crystallisation of the yellow material gave the complex $[\text{Cu}(\text{PNP}^{\text{NTPH}}\text{-Ph})\text{Cl}]$ (**1**) in almost 50% yield. We assume that it has been formed in a complex reaction including reduction of half of the Cu(II) to Cu(I) and oxidation of the ligand (Scheme 4A). Recrystallisation of the yellow material from EtOH yielded the pure complex and from the mother liquor we obtained blue crystals representing

the Cu(II) coordination polymer $[\text{Cu}(\text{O}_2\text{PPh}_2)_2]_n$ (**2**) which has been reported before.^[69–71] Diphenylphosphinate O_2PPh_2 is very probably the product of the assumed oxidation of the ligand and subsequent hydrolysis.

When reacting $\text{Cu}(\text{NO}_3)_2 \cdot 3\text{H}_2\text{O}$ with $\text{PNP}^{\text{NTPh}}\text{-Ph}$ in a 1:1 ratio in THF or acetone as solvents green solutions were obtained but no precipitation (Scheme 4B). Precipitation by adding *n*-hexane, diethyl ether or toluene was not successful. Evaporation to dryness followed by recrystallisation from EtOH, MeOH, THF, or MeCN did not yield a defined compound. Adding a few drops of pyridine to the reaction mixture lead to a violet precipitate. The material was soluble in DMF, DMSO, EtOH, or THF and insoluble in diethyl ether and *n*-hexane. A blue-green single crystal was obtained from a THF solution and represented the Cu(II) complex $[\text{Cu}(\text{O}_2\text{PPh}_2)_2(\text{Py})_2(\text{H}_2\text{O})]$ (**3**) containing two diphenylphosphinate, two pyridine, and one aqua ligand (Scheme 4B, for details on the structure, see later). The FT-IR spectrum of **3** clearly showed the absence of the triazine group band frequencies ($1500\text{--}1600\text{ cm}^{-1}$) and confirmed the hydrolysis of aminophosphine (NH–P) bonds. A strong absorption band at 1129 cm^{-1} represents the P=O stretch of the phosphinate ligand. The crystal and molecular structure of **3** is described below.

Another batch of blue-green crystals was later isolated from the above mentioned mother liquor and turned out to be the binuclear Cu(II) complex $[\text{Cu}(\text{O}_2\text{PPh}_2)(\text{NO}_3)(\text{Py})_2]_2$ (**4**) which also contains diphenylphosphinate ligands. Still another batch of crystals represented the new Cu(II) compound $[\text{Cu}(\text{Py})_4(\text{NO}_3)_2]\text{Py}$ (**5**).

From both reactions we concluded that after initial formation of the Cu(II) species $[\text{Cu}(\text{PNP}^{\text{NTPh}}\text{-Ph})(\text{X})_2]$ ($\text{X}=\text{Cl}$ or NO_3) the aminophosphine (NH–P) bonds of the PNP ligand were hydrolysed and the P atom is oxidised, while Cu(II) is reduced to Cu(I) in keeping with Bedford's report on the instability of $[\text{Cu}(\text{PNP}^{\text{Npy}}\text{-Ph})(\text{OAc})_2]$.^[48] In addition to this report, we were able to isolate and characterise the resulting Cu(I) complex $[\text{Cu}(\text{PNP}^{\text{NTPh}}\text{-Ph})\text{Cl}]$ (**1**) alongside with a number of Cu(II) by-products and side-products. The yield of **1** of approximately 50% means that half of the initially formed Cu(II) chlorido complex is reduced and this one-electron equivalent initiates the oxidation/hydrolysis of the PNP ligand. Unfortunately, we were not able to quantify the amount of oxidised products to balance the amounts of redox equivalents. The main product of the reaction of $\text{Cu}(\text{NO}_3)_2 \cdot 3\text{H}_2\text{O}$ with $\text{PNP}^{\text{NTPh}}\text{-Ph}$ and pyridine, the Cu(II) complex $[\text{Cu}(\text{O}_2\text{PPh}_2)_2(\text{Py})_2(\text{H}_2\text{O})]$ (**3**) was obtained in 62% yield. Moreover from the mother liquor another Cu(II) complexes **4** (13%) and **5** (traces) were obtained. Taken together with **3** this amounts to more than 75% of the material remaining in the Cu(II) oxidation state. At the same more than 32% of phosphinate O_2PPh_2 ligands resulted from the oxidation/hydrolysis of one equivalent of $\text{PNP}^{\text{NTPh}}\text{-Ph}$ ligand. This stands in stark contrast to the reaction with $\text{CuCl}_2 \cdot 2\text{H}_2\text{O}$ where at least half of the material was converted to Cu(I) and 50% of the $\text{PNP}^{\text{NTPh}}\text{-Ph}$ remained intact. From all this we concluded that the $\text{Cu}(\text{II})(\text{NO}_3)_2$ complex is more stable than the $\text{Cu}(\text{II})\text{Cl}_2$ homologue towards reduction and that the oxidation/

hydrolysis is not exclusively run by the Cu(II)/Cu(I) couple but probably also by O_2 as oxidant.

Trying to trace the initial Cu(II) complex the ligand $\text{PNP}^{\text{NTPh}}\text{-Ph}$ and $\text{Cu}(\text{NO}_3)_2 \cdot 3\text{H}_2\text{O}$ were ground in a mortar yielding a green powder which was washed rapidly with *n*-hexane and diethyl ether. Elemental analysis is in line with two NO_3 moieties per Cu. FT-IR show one distinctive vibration for the NO_3^- coligands in line with the formula $[\text{Cu}(\text{PNP}^{\text{NTPh}}\text{-Ph})(\text{NO}_3)_2]$ (**6**). An ESI-MS(+) peak at 681 might represent the species $[\text{Cu}(\text{PNP}^{\text{NTPh}}\text{-Ph})(\text{NO}_3) + \text{H}]^+$ (calc: 681). HR-ESI-MS(+) failed to give evidence for this species or the target complex. The X-band EPR spectrum of a powder sample showed a rhombic signal with approx. g values of $g_{\parallel}=2.315$, and $g_{\perp}=2.071$, coupling constants $A_{\parallel}=110\text{ G}$ and $A_{\perp}=55\text{ G}$ (Figure S17) in line with a Cu(II) species.^[72] Unfortunately we were not able to grow crystals of **6** as this compound is highly sensitive to moisture and air. The quite poor elemental analysis (see Experimental Part) underlines the rapid decomposition.

Hydrolysis of N–P bonds in similar PNP pincer bis-(phosphoramidite)pyridine ligands was reported previously, yielding Ni(II) and Pd(II) complexes containing phosphinite ligands (P in the oxidation state +III).^[26] In this report, the coordination of phosphine groups to Cu was supposed to enhance the electrophilicity of the P atoms making them more susceptible to nucleophilic attack.^[26] Interestingly, the bis-(diphenylphosphino)pyridine-2,6-diamine derivative used in the same study showed to tendency towards hydrolysis.^[26,28] Another similar hydrolysis was reported from a binuclear Au(I) complex of an *N,N*-(bis(diphenylphosphino)aniline) ligand.^[73] In this reaction yielding the P coordinated phosphinite $[\text{P}(\text{III})]$ complex $[\text{Au}(\text{P}(\text{O})\text{Ph}_2)\text{Cl}]$ and the aminophosphine complex $[\text{Au}(\text{PPh}_2\text{-NH-Ph-OMe})\text{Cl}]$ is initiated by fluoride anions and also here, no oxidation of a P atom occurs.^[73]

In our case, the hydrolysis in the reaction leads to phosphinate ligands (P in oxidation state +V) and for the pyridine plays an important role. So far we can only speculate and assume that pyridine acts as a base deprotonating the N–H amine group which triggers the hydrolysis + oxidation reaction, yielding diphenylphosphinate. Complexes of this ligand were described for Cr(III), Fe(III), Mn(II), Co(II), Ni(II), and UO_2^{2+} ^[74] and also Ag(I)^[75] and Cu(I).^[76] From Cu(II), so far only the homoleptic polymeric complex $[\text{Cu}(\text{O}_2\text{PPh}_2)_2]_n$ ^[69–71] and some mixed-ligand oligonuclear complexes such as $[\text{Cu}_4(\mu\text{-dppi})_4(\text{Hdppi})_2(\text{hfac})_4]$, $[\text{Cu}_5(\mu\text{-O})_2(\mu\text{-dppi})(\mu\text{-Hdppi})_2(\mu\text{-hfac})_3(\text{hfac})_2]$, and $[\text{Cu}_6(\mu\text{-O})_2(\mu\text{-dppi})_2(\mu\text{-Hdppi})(\mu\text{-hfac})_6]$ (Hdppi = diphenylphosphinic acid, hfac = hexafluoroacetylacetonate),^[77] have been described, but no simple heteroleptic Cu(II) complexes containing diphenylphosphinate.

Crystal and Molecular Structures

From the complexes $[\text{Cu}(\text{PNP}^{\text{NTPh}}\text{-Ph})\text{Cl}]$ (**1**) and $[\text{Cu}(\text{PNP}^{\text{NTPh}}\text{-Ph})(\text{NO}_3)_2]$ (**6**) no single crystals were obtained. Green-blue single crystals representing the compounds $[\text{Cu}(\text{O}_2\text{PPh}_2)_2]_n$ (**2**), $[\text{Cu}(\text{O}_2\text{PPh}_2)_2(\text{Py})_2(\text{H}_2\text{O})]$ (**3**), $[\text{Cu}(\text{O}_2\text{PPh}_2)(\text{NO}_3)(\text{Py})_2]$ (**4**), and $[\text{Cu}(\text{Py})_4(\text{NO}_3)_2]\text{Py}$ (**5**) were obtained from THF/pyridine solutions

(structural and refinement data in Tables S1 to S5). The crystal structure of **2** was found to crystallise in the space group $C2/c$ (No. 15), has been reported before^[69,70] and will thus not be further discussed.

The coordinated water molecule O5 in $[\text{Cu}(\text{O}_2\text{PPh}_2)_2(\text{Py})_2(\text{H}_2\text{O})]$ (**3**) forms intermolecular hydrogen bonds to the phosphorus oxide ions O2 and O4. This leads to the formation of chains parallel to the c -axis (Figure S14). The molecular structure of **3** (Figure 1, left) represents a square pyramidal $\text{trans-O}_2\text{N}_2$ coordination with the H_2O ligand occupying the axial position with an elongated Cu-O5 bond of 2.200(3) Å compared with the short basal Cu-N (2.047(4) and 2.049(4) Å) and Cu-O bonds (1.945(3) and 1.947(3) Å) (more data in Table S2, SI). The small basal angles were close to 90° (89.28(2) to 89.85(2)) but the large angles $\text{O}(1)\text{-Cu}(1)\text{-O}(3)$ and $\text{N}(1)\text{-Cu}(1)\text{-N}(2)$ lie about 170° showing that $\text{Cu}(1)$ is displaced from the centre of the square plane.

For $[\text{Cu}(\text{O}_2\text{PPh}_2)(\text{NO}_3)(\text{Py})_2]$ (**4**) no intermolecular interaction were found in the crystal structure (Figure S15). The dimeric molecular structure of **4** (Figure 1, right) shows two inversion-connected square-pyramidally coordinated Cu atoms. The basal plane is set by one short $\text{Cu-O5}_{\text{phosphinate}}$, a $\text{Cu-O2}_{\text{nitrate}}$ and two $\text{trans-Cu-N1}_{\text{pyridine}}$ and $\text{N2}_{\text{pyridine}}$ ligands. A further $\text{Cu-O5A}_{\text{phosphinate}}$ bond lies in the axial position. Remarkably, the elongation from the basal Cu-O5 bond of 1.955(1) Å to the axial Cu-O5A bond (2.149(1) Å) is only 11%.

The structure of $[\text{Cu}(\text{Py})_4(\text{NO}_3)_2]$ Py (**5**) was solved in $P2/n$ (No. 13). Intermolecular interactions were not found in the crystal structure (Figure S16). The molecular structure represent the frequently found coordination motive of a tetragonally elongated octahedron with short basal Cu-N distances of 1.995(3), 2.040(4), and 2.049(5) Å, respectively and markedly elongate axial Cu-O bonds of 2.443(2) Å ($\sim +20\%$). This is a new structure, but the metrics around Cu(II) are very similar to those in $[\text{Cu}(\text{Py})_4(\text{NO}_3)_2]2\text{Solv}$ (Solv = Py, THF, CHCl_3 or C_6H_6) (data in Table S2).^[78,79]

Electrochemistry of $\text{PNP}^{\text{NTPH}}\text{-Ph}$ and $[\text{Cu}(\text{PNP}^{\text{NTPH}}\text{-Ph})\text{Cl}]$

Cyclic voltammetry of the ligand $\text{PNP}^{\text{NTPH}}\text{-Ph}$ showed a first reversible (peak current ratio $I_{\text{pc}}/I_{\text{pa}} = 1$) and a second irreversible reduction wave (Figure 2) at -2.75 and -3.18 V, respectively. An intense oxidation (2 electrons) at $+1.04$ V was observed in the anodic range.

For the Cu(I) complex $[\text{Cu}(\text{PNP}^{\text{NTPH}}\text{-Ph})\text{Cl}]$ (**1**), two reduction waves and two oxidation waves were observed. Compared with the ligand the reductions of **1** are anodically shifted (less negative) which is in line with the assumption that for both the ligand and the complex the triazine unit harbours the lowest unoccupied molecular orbital (LUMO) and that coordination of Cu(I) facilitates the uptake of one electron in the reduction process. The large oxidation wave in the ligand presumably corresponds to the two $-\text{NH-PPh}_2$ units and the highest occupied molecular orbital of the ligand is located there. This wave is shifted to $+0.53$ V for the complex, while the anodic wave at $+0.11$ V very probably represents the $\text{Cu(I)} \rightarrow \text{Cu(II)}$ oxidation. The entire $\text{Cu(I)}/\text{Cu(II)}$ redox pair is represented by this anodic wave and two cathodic counter-waves at -0.04 and -0.44 V as measurements at different scan rates revealed (Figure 2, right, more figures in the SI). In total, this complex wave is completely reversible. This behaviour is typical for a $\text{Cu(I)}/\text{Cu(II)}$ couple and the geometrical reorganisation from the preferred tetrahedral geometry of a Cu(I) centre to square planar Cu(II) .^[80-83] Assuming a planar Cu(II) centre in the oxidised $[\text{Cu}(\text{PNP}^{\text{NTPH}}\text{-Ph})\text{Cl}]^+$ and a tetrahedral coordination of Cu(I) in $[\text{Cu}(\text{PNP}^{\text{NTPH}}\text{-Ph})\text{Cl}]$ (**1**) would be in line with a large re-arrangement. On the other hand the underlying re-arrangement could be the change from a trigonal or T-shaped geometry with three ligands (PPCl) around Cu(I) in **1** and a planar geometry of four-coordinate (PNPCL) Cu(II) in $[\mathbf{1}]^+$.

The geometry of the the Cu(I)Br complex $[\text{Cu}(\text{PNP}^{\text{NPy}}\text{-Ph})\text{Br}]$ ($\text{PNP}^{\text{NPy}}\text{-Ph} = N,N'$ -bis(diphenylphosphino)-2,6-di(methylamino)-pyridine)^[29] and of the cationic complexes $[\text{Cu}(\kappa^3\text{-PNP-PNP}^{\text{CPy}}\text{-Ph})\text{Cl}]$

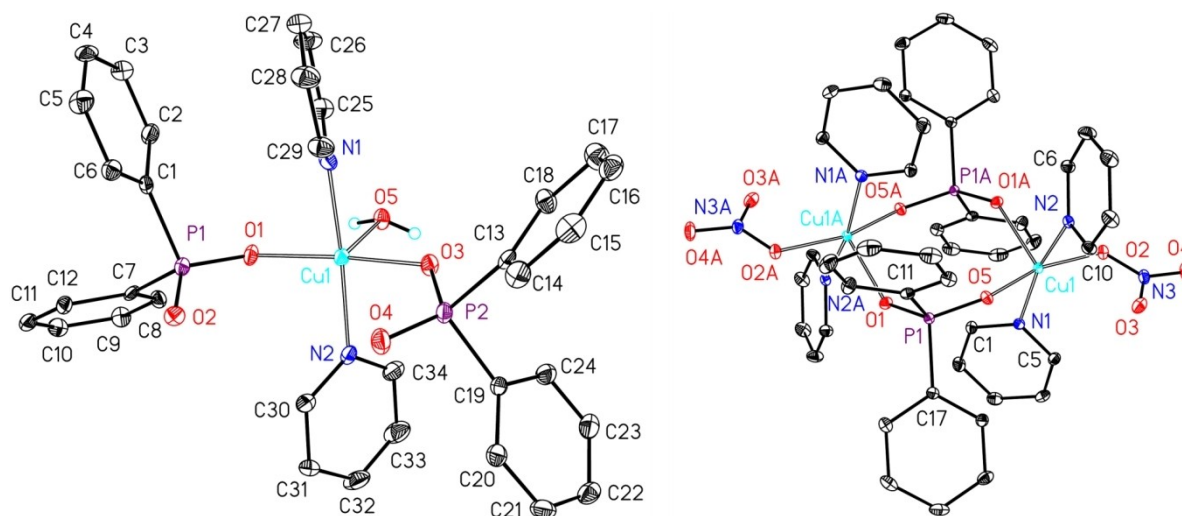


Figure 1. Molecular structures of $[\text{Cu}(\text{O}_2\text{PPh}_2)_2(\text{Py})_2(\text{H}_2\text{O})]$ (**3**) (left) and $[\text{Cu}(\text{O}_2\text{PPh}_2)(\text{NO}_3)(\text{Py})_2]$ (**4**) (right) with selected atom labelling. H atoms are omitted (with exception of the H_2O ligand in **3**) for clarity reasons. The ellipsoids represent a probability of 30%, H atoms are drawn with arbitrary radii.

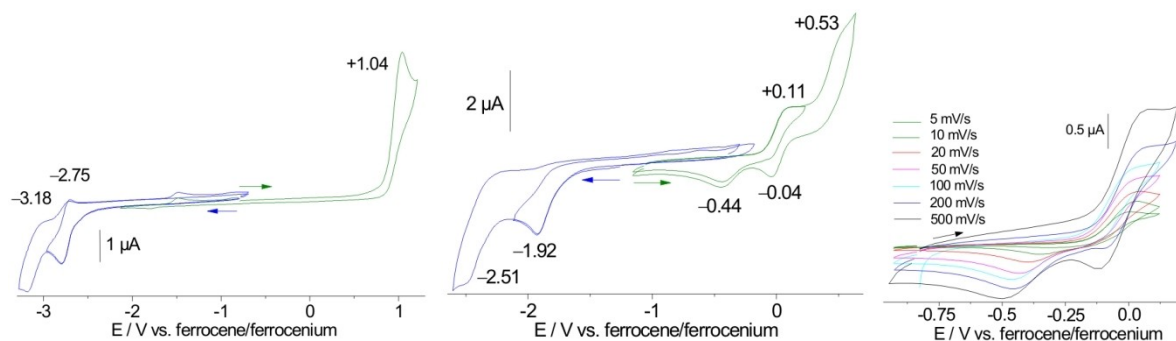


Figure 2. Cyclic voltammograms of PNP^{NTPH}-Ph (left) and [Cu(PNP^{NTPH}-Ph)Cl] (1) in THF/*n*Bu₄NPF₆ at 100 mV/s scan rate (middle) or at scan rates from 5 to 500 mV/s (right).

*t*Bu(L)]⁺ (L=PMe₃ or CN*t*Bu) adopt a distorted tetrahedral coordination around Cu(I).^[35] Recently the geometry of the complex [Zn(κ^3 -PNP-*PNP^{CPy}-*t*Bu)(Me)] (*PNP^{CPy}-*t*Bu = deprotonated 2,6-bis((di-*tert*-butylphosphanyl)methyl)pyridine) was shown to be tetrahedral around the Zn(II).^[30] These examples support our assumption that the PNP^{NTPH}-Ph ligand can adopt a tetrahedral coordination in the Cu(I) complex 1.

UV-vis absorption spectra recorded during thin-layer electrolysis (spectroelectrochemistry) of the complex 1 showed that during anodic oxidation an intense band at around 400 nm and a broad band centred at around 660 nm appeared (Figure 3, left). While the high-energy band is probably due to a ligand-(Cl)-to-metal(Cu) charge transfer (LMCT) transition, the long-wavelength band can be reorganisation assigned to the d-d ($t_{2g}^6 \rightarrow e_g^3$) transition of Cu(II) (d^9). This strongly supports the Cu(I) character of the complex 1 and the assignment of the first oxidation wave of 1 to the Cu(I)→Cu(II) oxidation. Cathodic reduction leads to growing bands at around 330 and 250 nm (Figure 3, right). As this energy range usually harbours the π - π^* transition of heteroaromatics such as triazine, we can assign this change to a reduction of the triazine unit.

From the electrochemical experiments we can conclude that the complex [Cu(PNP^{NTPH}-Ph)Cl] is clearly in oxidation state Cu(I). Concerning the intramolecular electron transfer in the

initial Cu(II) species [Cu(PNP^{NTPH}-Ph)X₂] (X=Cl⁻ or NO₃⁻) leading to Cu(I) and oxidised ligand fragments finally yielding the ⁻OOPPh₂ phosphinate ligands we can state that ligand oxidation occurs at relatively moderate potentials. The value of +1.04 V vs. ferrocene/ferrocenium translates into +0.22 vs Ag/AgCl, +0.48 V vs SCE, and +0.42 V vs NHE.^[84] Unfortunately, the already quite low oxidation potential of the PNP^{NTPH}-Ph ligand is markedly decreased by Cu(I) and probably not much less by Cu(II). The initially formed Cu(II) species [Cu(PNP^{NTPH}-Ph)X₂] adopt either a trigonal bipyramidal or a square pyramidal geometry which has a large impact on their Cu(II)/Cu(I) redox potential.^[80–83] The pair of similar Cu(II) complexes [Cu-(NNN^{NTPH}-Py)X₂] (NNN^{NTPH}-Py = *N,N'*-di(2-pyridyl)-2,4-diamino-6-phenyl-1,3,5-triazine; X=Cl⁻ or NO₃⁻) shows a rather perfect square pyramidal structure, while the NO₃ derivatives deviates towards trigonal bipyramidal.^[85] From this we assume that also the complexes [Cu(PNP^{NTPH}-Ph)X₂] (X=Cl⁻ or NO₃⁻) have different geometries and that for X=Cl the Cu(II)/Cu(I) redox pair lies at low (more negative) potential thus facilitating the electron transfer reaction from Cu(II) to the ligand in contrast to [Cu(PNP^{NTPH}-Ph)(NO₃)₂] (6) with a higher potential being more stable towards this intermolecular electron transfer. In this case air-borne O₂ is able to oxidise the ligand thus initialising the

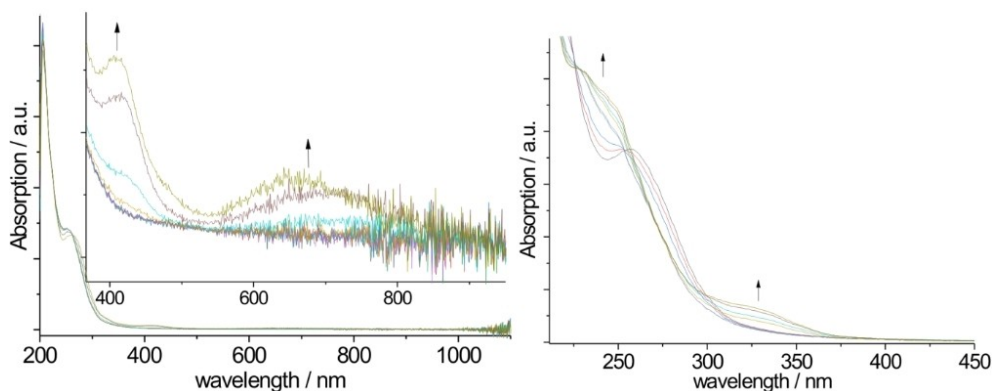


Figure 3. UV-vis absorption spectra recorded on solution of [Cu(PNP^{NTPH}-Ph)Cl] (1) in THF/*n*Bu₄NPF₆ during electrochemical oxidation (left) and reduction (right). The left plot represents a scan from -0.3 V to +0.1 V in steps of 20 mV. The right plot represents a scan from -1.5 to -2 V in steps of 50 mV.

oxidation/hydrolysis process converting PNP^{NTPH}-Ph to the phosphinate ligands without the conversion of Cu(II) to Cu(I).

Quite similar to our observations that Cu(II) and O₂ can oxidise the triazine based PNP^{NTPH}-Ph ligand with resulting formation of Cu(I) and oxidised ligand, the Cu(II) complex [Cu(Cy₂P(O)CH₂pyCH₂P(O)Cy₂)Cl(H₂O)]BF₄ was obtained from Cu(I) and the PNP^{Cy}-Cy (= 2,6-(dicyclohexylphosphinomethyl)-pyridine) ligand under exposure to air.^[31] In this example both Cu(I) and the ligand are oxidised in air leading to Cu(II) and a phosphineoxide ligand.

Catalytic activity of [Cu(PNP^{NTPH}-Ph)Cl] (1)

A first series of azide-alkyne click (AAC) reactions was carried out using benzyl bromide and phenylacetylene and an initial yield of 88% was obtained using a mixture of EtOH and H₂O (v:v = 1:1) using 1 mol% of the catalyst (1) (Table 1). Addition of sodium ascorbate did not improve the yield in line with the Cu(I) character of the catalyst. When the catalyst loading was decreased from 1 to 0.25 mol% the isolated yields gradually decreased from 88 to 83% (Table 1, entries 1–3) but heating and reduced reaction time restored a high yield of 97% (entry 6). Runs with H₂O or no solvent lead to 50% or no yield, respectively. Higher temperatures also lead to lower yields (entry 7).

The optimised reaction conditions were applied to varying substrates (Table 2). The use of benzyl bromide gives higher yields than the chloride (entries 1, 3, and 4) due to the better leaving group character of Br. and the introduction of a nitro group in the *ortho* reduces also the yield compared with the *para* derivative (entries 3 and 4) probably due to steric hindrance.

Analogous AAC catalysis experiments using the Cu(II) complex [Cu(O₂PPh₂)₂(Py)₂(H₂O)] (3) clearly showed that for this complex the reducing agent sodium ascorbate was mandatory. Using the same solvent mixture (EtOH/H₂O; 1:1), the optimisation of the reaction conditions (0.5 mol% catalyst, 70 °C, 60 min) allowed a yield of 85% (details in the SI).

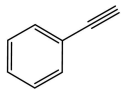
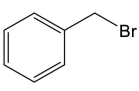
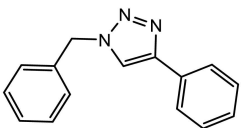
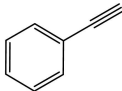
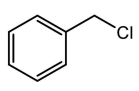
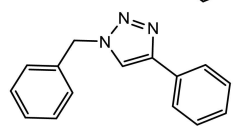
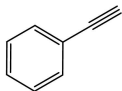
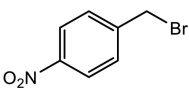
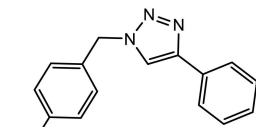
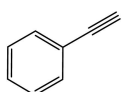
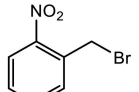
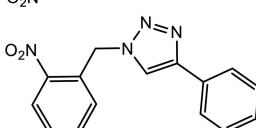
As 1-benzyl-4-phenyl-1*H*-1,2,3-triazole is a frequently used model compounds to assess catalysts for the AAC reaction we were able to compare our results with those of a number of other catalysts (Table 3). When comparing our Cu(II) precatalyst [Cu(PPh₂O₂)₂(Py)₂(H₂O)] (3) with other Cu(II) complexes (Table 3,

Table 1. Results of AAC reactions catalysed by [Cu(PNP^{NTPH}-Ph)Cl] (1) – optimisation.

Entry	Catalyst 1 [mol%]	Solvent	T [°C]	Time [min]	Yield [%] ^[a]
1	1	EtOH/H ₂ O (1:1)	r.t.	60	88
2	0.5	EtOH/H ₂ O (1:1)	r.t.	60	81
3	0.25	EtOH/H ₂ O (1:1)	r.t.	60	83
4	0.25	H ₂ O	r.t.	60	50
5	0.25	neat	r.t.	80	trace
6	0.25	EtOH/H ₂ O (1:1)	60	30	97
7	0.25	EtOH/H ₂ O (1:1)	85	30	78
8	none	EtOH/H ₂ O (1:1)	85	240	no product

[a] Isolated yield.

Table 2. Results of AAC reactions catalysed by [Cu(PNP^{NTPH}-Ph)Cl] (1) – substrate variation.

Entry	Alkyne	Aliphatic halide	Product	Time [min]	Yield [%] ^[a]
1				30	97
2				30	81
3				30	91
4				30	84

[a] Isolated yield.

Table 3. Catalytic activities of selected copper catalysts for the AAC reaction.

Entry	Catalyst <i>Homogeneous Cu(II)</i>	Catalyst load [mol%]	Further conditions	Yield [%]	Ref.
1	[Cu(O ₂ PPh ₂) ₂ (Py) ₂ (H ₂ O)] (3)	0.50	Na ascorb./EtOH:H ₂ O(1:1)/60 min/70 °C	85	this work
2	[CuL ₂] ^[a]	1.40	H ₂ O/12 h/70 °C	95	[57]
3	[Cu(phox) ₂] ^[b]	2.58	H ₂ O/12 h/70 °C	75	[58]
4	[Cu(Npy ₂ pz) ₂](PF ₆) ₂ ^[c,d]	0.10	Na ascorb./MeOH/16 h/r.t./N ₂ ^[e]	99	[87]
5	[CuL' ₂ (ONO) ₂] ^[d,f]	1.00	Na ascorb./EtOH:H ₂ O/10 min/r.t.	94	[88]
6	Cu(OTf) ₂ /IL ^[g,h]	0.10	Na ascorb./IL-PEG/60 min/r.t.	58	[89]
<i>Heterogeneous Cu(II)</i>					
7	[MNP _s @GLU][CuCl ₂] ^[i]	0.50	Na ascorb./H ₂ O/1 h/50 °C	99	[90]
8	Cu-PsIL ^[g,k]	0.20	Na ascorb./PEG-400/85 °C	99	[91]
9	PMMA-ONNO-Cu ^[d,l]	2.00	Na ascorb./EtOH/24 h/r.t./N ₂ ^[e]	98	[92]
10	MNP@ImAc/Cu ^[m]	0.20	Na ascorb./H ₂ O/1 h/r.t.	99	[93]
11	SNIL-Cu(OTf) ₂ ^[g,n]	0.05	Na ascorb./PEG/15 min/r.t.	75	[89]
<i>Homogeneous Cu(I)</i>					
12	[Cu(PNP ^{NTPh} -Ph)Cl] (1)	0.25	EtOH:H ₂ O(1:1)/30 min/60 °C	97	this work
13	[Cu(<i>o</i> NHC)Cl] ^[d,o]	1.00	neat/20 min/r.t.	99	[55]
14	[Cu(<i>ab</i> NHC)Cl] ^[d,p]	0.50	neat/2 h/r.t.	98	[94]
15	[Cu(SIMes)Cl] ^[d,q]	5.00	neat/30 min/r.t.	90–93	[95]
16	[CuBr(PPh(OPh) ₂)] ^[d]	0.50	H ₂ O/5.5 h/r.t.	> 95	[86]
17	[Cu(L ¹)Cl] ^[d,r]	0.50	acetone/20 h/r.t.	63	[96]
18	[Cu(L ¹) ₂](BF ₄) ^[d,r]	2.00	acetone/20 h/r.t.	57	[96]
19	[Cu(L ²)Cl] ^[d,s]	0.50	acetone/20 h/r.t.	92	[96]
20	[Cu(L ²) ₂](BF ₄) ^[d,s]	0.50	acetone/20 h/r.t.	< 95	[96]
21	[Cu(*PNP ^{CPy} -tBu)] ^[d,t]	1.00	Et ₂ O/16 h/60 °C/N ₂	40	[32]
22	[Cu(L ³)Cl] ^[d,u]	1.00	neat/4 h/r.t.	94	[97]
23	[Cu(L ³) ₂ Cl] ^[d,u]	2.00	H ₂ O/3 h/r.t.	96	[97]
24	[Cu(L ³) ₂ Cl] ^[d,u]	5.00	neat/0.5 h/r.t.	98	[97]
25	[Cu ₂ (bpoh)(PPh ₃) ₄] ^[v,w,x]	0.10	MeCN/3 h/r.t.	92	[98]
<i>Heterogeneous Cu(I)</i>					
26	MNP@[Cu(NNN ^{NT} -Py)] ^[v,w]	0.04	H ₂ O/2 h/50 °C	80	[99]
27	Fe ₃ O ₄ @SiO ₂ -caffeine-Cu(I)	0.36	H ₂ O/20 min/70 °C	96	[100]

[a] HL = 1-((4-bromophenylimino)methyl)naphthalen-2-ol; [b] Hphox = 2-(20-hydroxyphenyl)-2-oxazoline; [c] HNpy₂pz = N-bis[(pyridin-2-yl)methyl][1*H*-pyrazol-3-yl)methyl]amine; [d] Benzyl azide was used instead of NaN₃ and benzyl bromide; [e] Under an N₂ atmosphere; [f] L' = 5-acetyl-2-amino-6-methyl-4-(pyridin-3-yl)-4*H*-pyran-3-carbonitrile; [g] 4-bromo-benzylbromide was used; [h] IL = 4,4'-(ethane-1,2-diylbis(sulfanediyl))bis(1-methylpyridin-1-ium)iodide; [i] MNP = magnetic nano-particles, GLU = glucose; [k] PsIL = polystyrene supported ionic liquid; [l] PMMA = poly(methyl)(methacrylate)-supported ONNO Schiff base ligand; [m] MNP@ImAc = poly(ionic liquid)-coated magnetic nanoparticles; [n] SNIL = silica-nanoparticle-supported copper-containing ionic liquid; [o] *o*NHC = 1,3-bis(2,6-diisopropylphenyl)-2,4-diphenylimidazolylidene; [p] *ab*NHC = *N'*-diisopropylphenyl-*N*³-methyl-triazolylidene; [q] SIMes = 3-bis(2,4,6-trimethylphenyl)-4,5-dihydro-1*H*-3-imidazolylidene; [r] L¹ = *N,N'*-di(adamantan-1-yl)ethane-1,2-diimine; [s] L² = *N,N'*-dicyclohexylethane-1,2-diimine; [t] *PNP^{CPy}-tBu = deprotonated 2,6-di((*P*⁺Bu)₃methyl)pyridine; [u] L³ = 1,3-bis(2,6-dimethylphenyl)thiourea; [v] NNN^{NT}-Py = *N,N'*-di(pyridin-2-yl)-1,3,5-triazine-2,4,6-triamine; [w] Reaction of benzyl bromide, NaN₃ and ethyl-acetylenecarboxylate; [x] H₂bpoh = *N,N'*-bis(phenyl(pyridin-2-yl) methylene)oxalohydrazide.

entries 2–6) we can state a good performance for **3** (entry 6). Catalyst **3** definitely requires reduction using sodium ascorbate, presumably leading to a Cu(I) species, which is the active catalyst.^[32,53,54,56] This is in keeping with the report that the Cu(I) diphenyl-phosphinate complex [Cu(PPh(OPh)₂)Br] is an effective catalyst in AAC reactions (entry 16).^[86] Supported Cu(II) species have turned out to be very active after reduction using ascorbate (entries 7–11). The two Cu(II) complexes in entries 1 and 2,^[57] which are active in AAC without pre-treatment with a reductant, remain thus exclusive examples.

When compared to other Cu(I) based homogeneous catalysts (Table 3, entries 12–25), we can state that complex **1** is very suitable from several points of view. a) It is a stable Cu(I) complex and does not require activation of a Cu(II) pre-catalyst through reduction. b) Very high conversions or yields were

found in a reaction mixture of EtOH:H₂O which is environmentally much more benign than solvents such as acetone or acetonitrile. c) The catalyst **1** can be easily precipitated from the catalyst solution if required, as its solubility is generally low. This facile possibility of catalyst removal or recovery is superior to reactions run in neat reactants (entries 13–15, 22, 24).

At elevated temperatures, the catalyst **1** requires very short reaction times at very low catalyst load. Higher loads are needed at ambient temperature but also there, the reaction time was short. High temperatures and/or long reaction times were frequently found for other systems (entries 17–21) and were explained by the initial loss of a ligand, thus forming the active catalyst.^[32,96,97] From this we can thus conclude, that the Cu(I) precatalyst [Cu(PNP^{NTPh}-Ph)Cl] readily cleaves the Cl⁻ coli-

gand producing an undercoordinate Cu(I) species or is already in an undercoordinated *P,P,Cl* coordination (Scheme 3).

An interesting approach of an *in situ* synthesis of a $\text{Fe}_3\text{O}_4(\text{s})\text{-SiO}_2\text{-(CH}_2\text{)}_3\text{-}$ supported $[\text{Cu}(\text{PNP}^{\text{NT}}\text{-Py)}]_n$ AAC catalyst with very high catalytic activity was reported very recently (Table 3, entry 26).^[100] Unfortunately, no spectroscopic characterisation of the $[\text{Cu}(\text{PNP}^{\text{NT}}\text{-Py)}]$ entity, which resemble much to our catalyst 1, was provided.

Conclusions

The new Cu(I) complex $[\text{Cu}(\text{PNP}^{\text{NTPH}}\text{-PhCl)}]$ (1) containing the triazine-based $\text{PNP}^{\text{NTPH}}\text{-Ph}$ pincer ligand *N,N'*-bis-(diphenylphosphino)-2,6-diamino-4-phenyl-1,3,5-triazine was synthesised successfully from the PNP ligand and $[\text{Cu}(\text{SMe}_2)\text{Cl}]_n$ in good yields and was obtained alternatively from reaction solutions of the ligand and the Cu(II) precursor $\text{CuCl}_2\cdot 2\text{H}_2\text{O}$ in almost 50% yield. As side product of this reaction we observed the Cu(II) coordination polymer $[\text{Cu}(\text{O}_2\text{PPh}_2)_2]_n$ (2) containing diphenyl-phosphinate O_2PPh_2 as ligand resulting from an oxidation/hydrolysis reaction of the triazine pincer side groups -NH-PPh_2 . Using $\text{Cu}(\text{NO}_3)_2\cdot 3\text{H}_2\text{O}$ as precursor lead to solutions containing Cu(II) species and addition of pyridine allowed to isolate the Cu(II) phosphinate complexes $[\text{Cu}(\text{O}_2\text{PPh}_2)_2(\text{Py})_2(\text{H}_2\text{O})]$ (3) and $[\text{Cu}(\text{O}_2\text{PPh}_2)(\text{Py})_2(\text{NO}_3)_2]$ (4) alongside with $[\text{Cu}(\text{Py})_4(\text{NO}_3)_2]$ (5). We concluded that from the two initially formed Cu(II) complexes $[\text{Cu}(\text{PNP}^{\text{NTPH}}\text{-Ph)}\text{X}_2]$ with $\text{X}=\text{Cl}^-$ or NO_3^- the chlorido complex is rapidly undergoing $\text{Cu(II)}\rightarrow\text{Cu(I)}$ reduction thus initiating the oxidation/hydrolysis of the $\text{PNP}^{\text{NTPH}}\text{-Ph}$ ligand. The Cu(II) complex $[\text{Cu}(\text{PNP}^{\text{NTPH}}\text{-Ph})(\text{NO}_3)_2]$ (6) seemed to be more stable but could also not be isolated from the reaction solution. Instead we found the aforementioned phosphinate complexes 3 and 4 letting us conclude that also here the ligand $\text{PNP}^{\text{NTPH}}\text{-Ph}$ underwent the same oxidation/hydrolysis reaction sequence but the Cu(II)/Cu(I) redox couple was not the only driving force but also O_2 . Attempts to obtain 6 in a solid phase reaction gave good indication for this complex from ESI-MS and EPR spectroscopy but again, the material turned out highly sensitive to air and moisture preventing its isolation. But also the Cu(I) complex $[\text{Cu}(\text{PNP}^{\text{NTPH}}\text{-PhCl)}]$ (1) is very sensitive to hydrolysis (N-P bond) and oxidation (P atom). Thus, in the series of structurally similar PNP ligands, the 2,6-bis((PR'_2)methyl)pyridines ($\text{PNP}^{\text{CPY}}\text{-R}'$, Scheme 1 left), seem to be more stable in their Cu(I) complexes than the *N,N'*-bis(PR'_2)-2,6-diamino-pyridines ($\text{PNP}^{\text{NPY}}\text{-R}'$, Scheme 1, middle), and the herein studied *N,N'*-bis(PR'_2)-2,6-diamino-1,3,5-triazine ($\text{PNP}^{\text{NT}}\text{-R}'$) ligands. Cu(II) complexes of all three ligand types remain unreported, we only found some evidence for the complex $[\text{Cu}(\text{PNP}^{\text{NTPH}}\text{-Ph})(\text{NO}_3)_2]$ (6).

The Cu(I) complex $[\text{Cu}(\text{PNP}^{\text{NTPH}}\text{-PhCl)}]$ (1) was used as efficient catalyst for the azide-alkyne cycloaddition yielding various 1-benzyl-4-phenyl-1*H*-1,2,3-triazoles. Under optimised reaction condition 0.25 mol% catalyst were able to convert benzyl bromide and phenylacetylene to 1-benzyl-4-phenyl-1*H*-1,2,3-triazole in 97% yield in an EtOH:H₂O (1:1) solvent mixture in 30 min at moderate T of 60 °C making this catalyst superior

to a number of previously reported compounds. Catalysis experiments with $[\text{Cu}(\text{O}_2\text{PPh}_2)_2(\text{Py})_2(\text{H}_2\text{O})]$ (3) clearly showed that for this complex the reducing agent sodium ascorbate is mandatory but good yields were obtained.

Experimental Section

General: All manipulations of air and moisture sensitive compounds were performed under an inert atmosphere of Ar or N₂ using standard Schlenk techniques. THF was purified according to standard procedures and collected by distillation. THF and acetone were purchased from Daejung and Dr. Mojallali companies, respectively. All other chemicals were purchased from Merck and used as received. Fourier transform infrared (FT-IR) spectra were obtained in transmission mode using KBr pellets by a JASCO 680-PLUS spectrophotometer. ¹H NMR, ¹³C NMR, and ³¹P NMR spectra were recorded on a Bruker (DRX-400 MHz, ¹H: 400.13 MHz, ¹³C: 100.61), on a Bruker Avance II 300 MHz (¹H: 300 MHz, ¹³C: 75 MHz, ³¹P: 121.50 MHz) equipped with a double resonance (BBFO) 5 mm observe probehead with z-gradient coil, or a Bruker Avance III 500 MHz spectrometer with a narrow bore magnet (Bruker Spectrospin Ascend, 11.7 Tesla), using a TCI Prodigy 5 mm probe head with z-gradient. Elemental analysis was performed on a CHNSO Analyzer (Vario EL III) or a HEKAtech CHNS EuroEA 3000 Analyzer. Melting points were determined with IA9200 electrothermal apparatus. ESI-MS(+) was measured using a Thermo Finnigan TSQ 70 mass spectrometer, HR-ESI-MS(+) with a THERMO Scientific LTQ Orbitrap XL in the positive ion mode. EPR spectra were recorded in the X-band on a Bruker System ELEXSYS 500E equipped with a Bruker Variable Temperature Unit ER 4131VT (500 to 100 K); the *g* values were calibrated using a dpph sample. Electrochemical experiments were carried out in 0.1 M *n*Bu₄NPF₆ solutions using a three-electrode configuration (glassy carbon working electrode, Pt counter electrode, Ag/AgCl pseudo reference) and an Autolab PGSTAT30 potentiostat and function generator. Experiments were run at a scan rate of 100 mV/s at ambient temperature, the ferrocene/ferrocenium couple served as internal reference. UV-vis spectroelectrochemical measurements were performed with an optical transparent thin-layer electrochemical (OTTLE) cell.^[101,102]

Single Crystal X-ray Diffractometric Analysis: The intensity data for the compounds were collected on a Nonius Kappa CCD diffractometer using graphite-monochromated Mo- $\text{K}\alpha$ radiation. Data were corrected for Lorentz and polarisation effects; absorption was taken into account on a semi-empirical basis using multiple-scans.^[103-105] The structures were solved by direct methods (SHELXT)^[106] and refined by full-matrix least squares techniques against F_o^2 (SHELXL-2018).^[107] The hydrogen atoms bonded to the water molecule O5 atom of compound 3 were located by difference Fourier synthesis and refined isotropically. All other hydrogen atoms were included at calculated positions with fixed thermal parameters. The crystal of 5 was a non-merohedral twin. The twin law was determined by PLATON^[108] to (0.127 0.000 0.873) (0.000, -1.000, 0.000) (1.127 0.000 -0.127). The contribution of the main component were refined to 0.737(5). Additionally the crystal of 5 contains large voids, filled with disordered solvent molecules. The size of the voids is 221 Å³/unit cell. Their contribution to the structure factors was secured by back-Fourier transformation using the SQUEEZE routine of the program PLATON^[108] resulting in 89 electrons/unit cell. The crystal of 3 was refined as a 2-component inversion twin. All non-hydrogen atoms were refined anisotropically.^[107] XP^[109] was used for structure representations. Crystallographic data as well as structure solution and refinement details are summarised in Table S1, SI.

Syntheses

Synthesis of the ligand PNP^{NTPH}-Ph: The ligand was synthesised from 2,6-diamino-4-phenyl-1,3,5-triazine (0.5 g, 2.67 mmol), PPh₂Cl (0.96 mL, 5.34 mmol) and NEt₃ (0.82 mL, 5.88 mmol) in THF solution following a literature procedure.^[28] ¹H NMR (400 MHz, C₆D₆): δ = 7.46–7.00 (m, 25H, Ph and PPh), 6.34 (s, 2H, NH) ppm. ¹H NMR (400 MHz, MeCN-*d*₃): δ = 8.24–8.34 (m, 1H), 7.90–7.70 (m, 1H), 7.64–7.23 (m, 23H), 6.69 (s, br, 2H, NH) ppm. ³¹P{¹H} NMR (162 MHz, C₆D₆): δ = 27.4 ppm (29.3 ppm reported from ref. [28]). ³¹P{¹H} NMR (121.5 MHz, MeCN-*d*₃): δ = 26.3 ppm. ³¹P{¹H} NMR (121.5 MHz, DMSO-*d*₆): δ = 27.6 ppm.

Synthesis of [Cu(PNP^{NTPH}-Ph)Cl]·0.5 Et₂O (1·0.5Et₂O): [Cu(SMe₂)Cl]_n (68 mg, 0.4 mmol) was dissolved in warm acetone (10 mL) and PNP^{NTPH}-Ph (222 mg, 0.4 mmol) was added. After 1 hour of stirring a yellow precipitate was formed which was filtered off, washed twice with Et₂O and dried under vacuum. Yield: 228 mg (0.33 mmol, 82%). Anal. Calc. for C₃₃H₂₇N₅P₂CuCl·0.5(C₄H₁₀O) (691.61 g/mol): C, 60.78; H, 4.66; N, 10.13. Found: C, 60.76; H, 4.66; N, 10.33%. ¹H NMR (300 MHz, DMSO-*d*₆): δ = 8.40–8.20 (m, 2H), 8.00–7.30 (m, 25H) ppm. Further signals at 3.38 (q, 1H) and 1.09 (t, 1.5H) were assigned to co-crystallised diethyl ether, while signals at 3.09 (q, 1H) and 1.18 (q, 1.5H) seem to be coordinated diethyl ether. The total amount of Et₂O is 0.5 equivalents. ¹H NMR (499 MHz, MeCN-*d*₃): δ = 8.35–8.27 (m, 1H), 8.02–7.94 (m, 1H), 7.90–7.29 (m, 25H) ppm. Further signals at 3.42 (q, 2H) and 1.12 (t, 3H) were assigned to co-crystallised diethyl ether (0.5 equivalents). ³¹P{¹H} NMR (121.5 MHz, DMSO-*d*₆): δ = 15.6 ppm. ³¹P{¹H} NMR (121.5 MHz, MeCN-*d*₃): δ = 21 ppm.

Synthesis of [Cu(PNP^{NTPH}-Ph)Cl] (1): CuCl₂·2H₂O (68 mg, 0.4 mmol) was dissolved in warm acetone (10 mL) and PNP^{NTPH}-Ph (222 mg, 0.4 mmol) was added. After 1 hour of stirring a yellow precipitate was formed which was filtered off, washed twice with Et₂O and dried under vacuum. Yield: 140 mg (51%). Anal. Calc. for C₃₃H₂₇N₅P₂CuCl (654.55 g/mol): C, 60.55; H, 4.16; N, 10.70. Found: C, 60.66; H, 4.16; N, 10.73%. FT-IR (KBr, cm⁻¹): 3388 (w, ν N–H), 3051(m), 1597, 1536 (vs, ν triazine), 1486 (m), 1449 (s), 1427 (s), 1401 (s), 1179 (m), 1101 (m, ν N–P), 693 (s), 519 (m), 484 (w). HR-ESI-MS(+): 653.07258 (calculated for [M]⁺: 653.07262); 618.10348 (calculated for [M–Cl]⁺: 618.10377) m/z.

Synthesis of [Cu(O₂PPh₂)₂(Py)₂(H₂O)] (3): To a solution of 48 mg (0.2 mmol) Cu(NO₃)₂·3H₂O in 5 mL THF 111 mg (0.2 mmol) of PNP^{NTPH}-Ph was added whereupon the colour of the solution immediately turned to deep green. Then, two drops of pyridine were added and a violet precipitate was formed. The mixture was stirred at room temperature for 1 h. Then the violet precipitate was filtered off, washed twice with cold THF, and dried under vacuum, yielding 83 mg (0.12 mmol, 62%) of a violet solid. Anal. Calc. for C₃₄H₃₀N₂O₅P₂Cu (672.12 g/mol): C, 60.76; H, 4.50; N, 4.17. Found: C, 60.70; H, 4.51; N, 4.19%. FT-IR (KBr, cm⁻¹): 3405 (w), 3025 (w), 3012 (w, ν C–H), 1464 (s), 1436 (s), 1129 (vs, ν P=O), 1052 (s), 1024 (s), 997 (m), 752 (m), 727 (s), 695 (s), 573 (s), 545 (m), 470 (w), 436 (w).

Synthesis of [Cu(O₂PPh₂)(NO₃)(Py)₂] (4) and [Cu(Py)₄(NO₃)₂] (5): Leaving the mother liquor of the above reaction procedure for about 14 days allowed to collect 27 mg (0.027 mmol, 13%) of blue-green crystals of 4 and after further 48 days a few crystals of 5. Anal. Calc. for C₄₄H₃₆N₆O₁₀P₂Cu (997.84 g/mol): C, 52.96; H, 3.64; N, 8.42. Found: C, 52.90; H, 3.61; N, 8.33%.

Attempted synthesis of [Cu(PNP^{NTPH}-Ph)(NO₃)₂] (6): The ligand PNP^{NTPH}-Ph (55 mg, 0.1 mmol) and Cu(NO₃)₂·3H₂O (24.2 mg, 0.1 mmol) were ground carefully in an agate mortar for 30 min yielding a green powder. This was washed rapidly with small portions of *n*-hexane and diethyl ether and then dried. Anal. Calc. for C₃₃H₂₇N₇O₆P₂Cu (743.11 g/mol): C, 53.34; H, 3.66; N, 13.19. Found:

C, 54.70; H, 3.61; N, 11.75%. ESI-MS(+): 681 m/z [Cu(PNP^{NTPH}-Ph)(NO₃)₂ + H]⁺. HR-ESI-MS(+): gave no match with the calculated values for [M]⁺: 742.07940.07262, or [M–NO₃]⁺: 680.09158 m/z.

General procedure for the catalysis yielding the 1,2,3-triazoles: Predefined amounts of catalysts (see Tables 1, 2, S6 and S7), benzyl halide (1 mmol), sodium azide (1.2 mmol), alkyne (1 mmol), and solvent (2 mL) were placed in a screw cap vial. The reaction mixture was stirred at room temperature and the progress of the reaction was monitored by TLC (eluent: ethyl acetate/*n*-hexane 3:10). The product was extracted with ethyl acetate (25 mL) from the aqueous phase. Organic phases were passed through 1 cm silica gel column for removal of the catalysts. Then, the solutions were evaporated to dryness under reduced pressure to give the corresponding 1,2,3-triazoles.

Benzyl-4-phenyl-1H-1,2,3-triazole: Mp: 128–130 °C. ¹H NMR (400 MHz, CDCl₃): δ = 5.6 (s, 2H), 7.32–7.36 (m, 3H), 7.39–7.44 (m, 5H), 7.74 (s, 1H), and 7.84 (d, *J* = 8 Hz, 2H). ¹³C NMR (100 MHz, CDCl₃): δ = 54.3, 125.7, 128.1, 128.2, 128.8, 128.8, 129.2, 130.6, 134.7, and 150.1. FT-IR (KBr, cm⁻¹): 3121 (m), 1466 (m), 1357 (w), 1224 (m), 1075 (m), 1049 (m), 766 (s), 766 (s), 693 (s).

1-(4-nitrobenzyl)-4-phenyl-1H-1,2,3-triazole: Mp: 154–155 °C. ¹H NMR (400 MHz, CDCl₃): δ = 5.72 (s, 2H), 7.32–7.41 (m, 1H), 7.41–7.52 (m, 4H), 7.78 (s, 1H), 7.84 (d, *J* = 7.2 Hz, 2H), 8.26 (d, *J* = 8.7 Hz, 2H). ¹³C NMR (100 MHz, CDCl₃): δ = 53.2, 116.4, 124.4, 125.8, 128.5, 128.6, 128.9, 130.1, 141.7, 148.1. FT-IR (KBr, cm⁻¹): 3127 (w), 1609 (w), 1516 (s), 1348 (s), 1073 (m), 861 (w), 765 (m), 514 (w).

1-(2-nitrobenzyl)-4-phenyl-1H-1,2,3-triazole: ¹H NMR (400 MHz, CDCl₃): δ = 6.02 (s, 2H), 7.17 (d, *J* = 7.5 Hz, 1H), 7.37 (t, *J* = 7.4 Hz, 1H), 7.45 (dd, *J*_{av} = 7.5 Hz, 2H), 7.56 (dd, *J*_{av} = 7.7 Hz, 1H), 7.64 (dd, *J*_{av} = 7.6 Hz, 1H), 7.87 (d, *J*_{av} = 7.1 Hz, 2H), 7.96 (s, 1H), 8.19 (d, *J* = 8.1 Hz, 1H). ¹³C NMR (100 MHz, CDCl₃): δ = 50.9, 120.6, 125.4, 125.8, 128.4, 128.9, 129.7, 130.2, 130.3, 130.8, 134.4, 148.4.

Deposition Numbers 2041103 (for 3), 2041104 (for 4), and 2041105 (for 5) contain the supplementary crystallographic data for this paper. These data are provided free of charge by the joint Cambridge Crystallographic Data Centre and Fachinformationszentrum Karlsruhe Access Structures service www.ccdc.cam.ac.uk/structures.

Supporting Information

(see footnote on the first page of this article): The following are available online: NMR, FT-IR and HR-ESI-MS spectra of [Cu(PNP^{NTPH}-Ph)Cl]·0.5Et₂O (1·0.5Et₂O) and of the material obtained from Cu(NO₃)₂·3H₂O and PNP^{NTPH}-Ph in solution, crystal structures of [Cu(O₂PPh₂)₂(Py)₂(H₂O)] (3), [Cu(O₂PPh₂)(NO₃)(Py)₂] (4), and [Cu(Py)₄(NO₃)₂] (5) with atom labelling, an X-band EPR spectrum of the material obtained through grinding PNP^{NTPH}-Ph and Cu(NO₃)₂·3H₂O, cyclic voltammograms of 1, together with Supplementary Tables S1–S5 containing crystal structure and refinement data of all compounds and Tables S6 and S7 collecting AAC catalytic data for complex 3.

Author Contributions

G.M. designed the project, supervised the preparative and characterisation work and wrote the manuscript draft. A.M.A. and S.S. did the syntheses, characterisation and catalysis. H.G.

and W.P. collected XRD data, solved the structures and provided figures and tables. A.S. did the electrochemical experiments. A.K. designed and supervised the project, provided equipment and revised the manuscript. All authors have read and agreed to the submitted version of the manuscript.

Acknowledgements

Prof. Dr. Mathias Schäfer and Michael Neihls, Department of Chemistry, University of Cologne are acknowledged for the HR-ESI-MS measurements. We also thank Alexander Haseloer for the EPR simulation. **Funding:** G.M. gratefully acknowledges the Iran National Science Foundation (INSF) for supporting this study (94006007). Partial financial support from the Research Affairs Division of Isfahan University of Technology (IUT), Iran, is also acknowledged. A.K., W.P. and G.M. thank the Deutsche Forschungsgemeinschaft (DFG) for the Initiation of International Collaboration grants KL-1194/17-1 and PL-155/17-1. A.K. thanks the German Academic Exchange Service (DAAD) for a short-term short-time guest lectureship KD-0001052598-2 and the University of Shiraz, Iran for support. Open access funding enabled and organized by Projekt DEAL.

Conflict of Interest

The authors declare no conflict of interest.

Keywords: Copper · PNP pincer ligands · Redox chemistry · Spectroelectrochemistry · Azide click reaction

- [1] M. Albrecht, G. van Koten, *Angew. Chem. Int. Ed.* **2001**, *40*, 3750–3781.
- [2] G. van Koten, Gerard, R. A. Gossage, *The Privileged Pincer-Metal Platform: Coordination Chemistry & Applications*. (Eds.). Series Topics in Organometallic Chemistry, Springer, Heidelberg, Berlin **2016**.
- [3] S. Werkmeister, J. Neumann, K. Junge, M. Beller, *Chem. Eur. J.* **2015**, *21*, 12226–12250.
- [4] C. Gunanathan, D. Milstein, *Chem. Rev.* **2014**, *114*, 12024–12087.
- [5] C. Gunanathan, D. Milstein, *Acc. Chem. Res.* **2011**, *44*, 588–602.
- [6] J. Choi, A. H. Roy MacArthur, M. Brookhart, A. S. Goldman, *Chem. Rev.* **2011**, *111*, 1761–1779.
- [7] L. Alig, M. Fritz, S. Schneider, *Chem. Rev.* **2019**, *119*, 2681–2751.
- [8] H. Li, T. P. Gonçalves, D. Lupp, K.-W. Huang, *ACS Catal.* **2019**, *9*, 1619–1629.
- [9] H. Li, B. Zheng, K.-W. Huang, *Coord. Chem. Rev.* **2015**, *293–294*, 116–138.
- [10] G. L. Parker, S. Lau, B. Leforestier, A. B. Chaplin, *Eur. J. Inorg. Chem.* **2019**, 3791–3798.
- [11] T. Zell, D. Milstein, *Acc. Chem. Res.* **2015**, *48*, 1979–1994.
- [12] S. Schneider, J. Meiners, B. Askevold, *Eur. J. Inorg. Chem.* **2012**, *2012*, 412–429.
- [13] C. Müller, E. A. Pidko, M. Lutz, A. L. Spek, D. Vogt, *Chem. Eur. J.* **2008**, *14*, 8803–8807.
- [14] D. Benito-Garagorri, K. Kirchner, *Acc. Chem. Res.* **2008**, *41*, 201–213.
- [15] J. I. van der Vlugt, in *Copper(I) chemistry of phosphines, functionalized phosphines, and phosphorus heterocycles*, (Ed.: M. S. Balakrishna), Elsevier, Amsterdam, **2019**, vol. 6, pp. 145–163.
- [16] C. Schröder-Holzhaecker, B. Stöger, E. Pittenauer, G. Allmaier, L. F. Veiros, K. Kirchner, *Monatsh. Chem.* **2016**, *147*, 1539–1545.
- [17] M. Mastalir, E. Pittenauer, B. Stöger, G. Allmaier, K. Kirchner, *Org. Lett.* **2017**, *19*, 2178–2181.
- [18] D. Benito-Garagorri, J. Wiedermann, M. Pollak, K. Mereiter, K. Kirchner, *Organometallics* **2007**, *26*, 217–222.
- [19] M. Mastalir, B. Stöger, E. Pittenauer, M. Puchberger, G. Allmaier, K. Kirchner, *Adv. Synth. Catal.* **2016**, *358*, 3824–3831.
- [20] F. Freitag, T. Irrgang, R. Kempe, *Chem. Eur. J.* **2017**, *23*, 12110–12113.
- [21] N. Deibl, R. Kempe, *J. Am. Chem. Soc.* **2016**, *138*, 10786–10789.
- [22] S. Rösler, M. Ertl, T. Irrgang, R. Kempe, *Angew. Chem., Int. Ed.* **2015**, *54*, 15046–15050.
- [23] S. Rösler, J. Obenauf, R. Kempe, *J. Am. Chem. Soc.* **2015**, *137*, 7998–8001.
- [24] M. Mastalir, K. Kirchner, *Monatsh. Chem.* **2017**, *148*, 105–109.
- [25] M. Mastalir, B. Stöger, E. Pittenauer, G. Allmaier, K. Kirchner, *Org. Lett.* **2016**, *18*, 3186–3189.
- [26] D. Benito-Garagorri, K. Mereiter, K. Kirchner, *Eur. J. Inorg. Chem.* **2006**, *21*, 4374–4379.
- [27] P. Arce, C. Vera, D. Escudero, J. Guerrero, A. Lappin, A. Oliver, D. H. Jara, G. Ferraudi, L. Lemus, *Dalton Trans.* **2017**, *46*, 13432–13445.
- [28] D. Benito-Garagorri, E. Becker, J. Wiedermann, W. Lackner, M. Pollak, K. Mereiter, J. Kisala, K. Kirchner, *Organometallics* **2006**, *25*, 1900–1913.
- [29] G. K. Rao, S. I. Gorelsky, I. Korobkov, D. Richeson, *Dalton Trans.* **2015**, *44*, 19153–19162.
- [30] M. Rauch, S. Kar, A. Kumar, L. Avram, L. J. W. Shimon, D. Milstein, *J. Am. Chem. Soc.* **2020**, *142*, 14513–14521.
- [31] H.-F. Lang, P. E. Fanwick, R. A. Walton, *Inorg. Chim. Acta* **2002**, *329*, 9–12.
- [32] S. Y. de Boer, Y. Gloaguen, M. Lutz, J. I. van der Vlugt, *Inorg. Chim. Acta* **2012**, *380*, 336–342.
- [33] J. I. van der Vlugt, E. A. Pidko, R. C. Bauer, Y. Gloaguen, M. K. Rong, M. Lutz, *Chem. Eur. J.* **2011**, *17*, 3850–3854.
- [34] J. I. van der Vlugt, E. A. Pidko, D. Vogt, M. Lutz, A. L. Spek, *Inorg. Chem.* **2009**, *48*, 7513–7515.
- [35] J. I. van der Vlugt, E. A. Pidko, D. Vogt, M. Lutz, A. L. Spek, A. Meetsma, *Inorg. Chem.* **2008**, *47*, 4442–4444.
- [36] T. Hille, T. Irrgang, R. Kempe, *Chem. Eur. J.* **2014**, *20*, 5569–5572.
- [37] S. Michlik, R. Kempe, *Angew. Chem. Int. Ed.* **2013**, *52*, 6326–6329.
- [38] S. Michlik, R. Kempe, *Nat. Chem.* **2013**, *5*, 140–144.
- [39] S. Qu, Y. Dang, C. Song, M. Wen, K.-W. Huang, Z.-X. Wang, *J. Am. Chem. Soc.* **2014**, *136*, 4974–4991.
- [40] R. Fertig, T. Irrgang, F. Freitag, J. Zander, R. Kempe, *ACS Catal.* **2018**, *8*, 8525–8530.
- [41] G. Zhang, T. Irrgang, T. Dietel, F. Kallmeier, R. Kempe, *Angew. Chem. Int. Ed.* **2018**, *57*, 9131–9135.
- [42] F. Kallmeier, B. Dudzic, T. Irrgang, R. Kempe, *Angew. Chem. Int. Ed.* **2017**, *56*, 7261–7265.
- [43] F. Kallmeier, T. Irrgang, T. Dietel, R. Kempe, *Angew. Chem. Int. Ed.* **2016**, *55*, 11806–11809.
- [44] M. Koley, K. Kirchner, K. Mereiter, *Acta Crystallogr. Sect. E* **2011**, *67*, m1842–1843.
- [45] G. Wang, Z. Li, C. Li, S. Zhang, *Chem. Eng. J.* **2019**, *359*, 863–873.
- [46] M. Schlagbauer, F. Kallmeier, T. Irrgang, R. Kempe, *Angew. Chem. Int. Ed.* **2020**, *59*, 1485–1490.
- [47] L. M. Kumar, R. M. Ansari, B. R. Bhat, *Appl. Organomet. Chem.* **2018**, *32*, e4054 (1–8).
- [48] S. B. Tailor, M. Manzotti, S. Asghar, B. J. S. Rowsell, S. L. J. Luckham, H. A. Sparkes, R. B. Bedford, *Organometallics* **2019**, *38*, 1770–1777.
- [49] Z. Pan, M. T. Gamer, P. W. Roesky, *Z. Anorg. Allg. Chem.* **2006**, *632*, 744–748.
- [50] K. Takeuchi, Y. Tanaka, I. Tanigawa, F. Ozawa, J.-C. Choi, *Dalton Trans.*, **2020**, *49*, 3630–3637.
- [51] H. C. Kolb, M. G. Finn, K. B. Sharpless, *Angew. Chem. Int. Ed.* **2001**, *40*, 2004–2021.
- [52] T. M. A. Barlow, D. Tourwé, S. Ballet, *Eur. J. Org. Chem.* **2017**, *2017*, 4678–4694.
- [53] Z.-J. Zheng, D. Wang, Z. Xu, L.-W. Xu, *Beilstein J. Org. Chem.* **2015**, *11*, 2557–2576.
- [54] A. Mandoli, *Molecules* **2016**, *21*, 117 (1–43).
- [55] S. C. Sau, S. R. Roy, T. K. Sen, D. Mullangi, S. K. Mandal, *Adv. Synth. Catal.* **2013**, *355*, 2982–2991.
- [56] N. Noshiranzadeh, M. Emami, R. Bikas, A. Kozakiewicz, *New J. Chem.* **2017**, *41*, 2658–2667.
- [57] M. Bagherzadeh, A. Bayrami, R. Kia, M. Amini, L. J. K. Cook, P. R. Raithby, *Inorg. Chim. Acta* **2017**, *466*, 398–404.
- [58] B. S. P. A. Kumar, K. H. V. Reddy, K. Karnakar, G. Satish, Y. V. D. Nageswar, *Tetrahedron Lett.* **2015**, *56*, 1968–1972.

- [59] L. Cao, C. Liu, X. Tang, X. Yin, B. Zhang, *Tetrahedron Lett.* **2014**, *55*, 5033–5037.
- [60] A. Akbari, N. Arsalani, M. Amini, E. Jabbari, *J. Mol. Catal. A* **2016**, *414*, 47–54.
- [61] Y. Jiang, D. Kong, J. Zhao, W. Zhang, W. Xu, W. Li, G. Xu, *Tetrahedron Lett.* **2014**, *55*, 2410–2414.
- [62] B. Kaboudin, R. Mostafalu, T. Yokomatsu, *Green Chem.* **2013**, *15*, 2266–2274.
- [63] S. Bahadorikhalili, L. Ma'mani, H. Mahdavi, A. Shafiee, *Microporous Mesoporous Mater.* **2018**, *262*, 207–216.
- [64] C. Nájera, J. M. Sansano, *Org. Biomol. Chem.* **2009**, *7*, 4567–4581.
- [65] D. Dheer, V. Singh, R. Shankar, *Bioorg. Chem.* **2017**, *71*, 30–54.
- [66] B. Zhang, *Eur. J. Med. Chem.* **2019**, *168*, 357–372.
- [67] K. Bozorov, J. Zhao, H. A. Aisa, *Bioorg. Med. Chem.* **2019**, *27*, 3511–3531.
- [68] J. I. van der Vlugt, M. A. Siegler, M. Janssen, D. Vogt, A. L. Spek, *Organometallics* **2009**, *28*, 7025–7032.
- [69] K. Gholivand, N. Fallah, A. A. E. Valmoozi, A. Gholami, M. Dusek, V. Eigner, M. Pooyan, F. Mohammadpanah, *J. Mol. Struct.* **2020**, *1202*, 127369.
- [70] A. Bino, L. Sissman, *Inorg. Chim. Acta* **1987**, *128*, L21–L22.
- [71] J.-L. Du, K. W. Oliver, R. C. Thompson, *Inorg. Chim. Acta* **1988**, *141*, 19–20.
- [72] P. H. Rieger, *Electron Spin Resonance – Analysis and Interpretation*, RSC Publishing, Cambridge, UK, **2007**.
- [73] X. He, W. H. Lam, E. C.-C. Cheng, V. W.-W. Yam, *Chem. Eur. J.* **2015**, *21*, 8447–8454.
- [74] I. Rosca, D. Sutiman, A. Căilean, M. Vizitiu, I. Rusu, D. Sibiescu, *Thermochim. Acta* **1995**, *269/270*, 295–305.
- [75] N. Kuhn, A. Voss, E. Zauder, P. Sartori, *Chem.-Ztg.* **1982**, *106*, 299–300.
- [76] Y. Liu, C. S. Diercks, Y. Ma, H. Lyu, C. Zhu, S. A. Alshmiri, S. Alshihri, O. M. Yaghi, *J. Am. Chem. Soc.* **2019**, *141*, 677–683.
- [77] S. Calancea, S. G. Reis, G. P. Guedes, R. A. A. Cassaro, F. Semaan, F. López-Ortiz, M. G. F. Vaz, *Inorg. Chim. Acta* **2016**, *453*, 104–114.
- [78] D. V. Soldatov, G. D. Enright, J. A. Ripmeester, J. Lipkowski, E. A. Ukraintseva, *J. Supramol. Chem.* **2001**, *1*, 245–251.
- [79] E. A. Ukraintseva, V. A. Logvinenko, D. V. Soldatov, T. A. Chingina, *J. Therm. Anal. Calorim.* **2004**, *75*, 337–345.
- [80] W. Kaim, J. Rall, *Angew. Chem., Int. Ed.* **1996**, *35*, 43–60.
- [81] H. Nagao, N. Komeda, M. Mukaida, M. Suzuki, K. Tanaka, *Inorg. Chem.* **1996**, *35*, 6809–6815.
- [82] J. Schnödt, J. Manzur, A.-M. García, I. Hartenbach, C.-Y. Su, J. Fiedler, W. Kaim, *Eur. J. Inorg. Chem.* **2011**, *2011*, 1436–1441.
- [83] M. Bubrin, H. Kvapilová, J. Fiedler, F. Ehret, S. Zálaiš, W. Kaim, *Z. Anorg. Allg. Chem.* **2018**, *644*, 661–670.
- [84] N. G. Connelly, W. E. Geiger, *Chem. Rev.* **1996**, *96*, 877–910.
- [85] C. J. Wang, Y. Y. Wang, H. R. Ma, H. Wang, Q. Z. Shi, S. M. Peng, *Polyhedron* **2006**, *25*, 195–202.
- [86] S. Lal, J. McNally, A. J. P. White, S. Díez-González, *Organometallics* **2011**, *30*, 6225–6232.
- [87] B. Han, X. Xiao, L. Wang, W. Ye, X. Liu, *Chin. J. Catal.* **2016**, *37*, 1446–1450.
- [88] M. Bihani, B. G. Pasupuleti, P. P. Bora, G. Bez, R. A. Lal, *Catal. Lett.* **2018**, *148*, 1315–1323.
- [89] M. Tavassoli, A. Landarani-Isfahani, M. Moghadam, S. Tangestaninejad, V. Mirkhani, I. Mohammadpoor-Baltork, *ACS Sustainable Chem. Eng.* **2016**, *4*, 1454–1462.
- [90] F. M. Moghaddam, V. Saberi, S. Kalhor, S. E. Ayati, *RSC Adv.* **2016**, *6*, 80234–80243.
- [91] M. Tavassoli, A. Landarani-Isfahani, M. Moghadam, S. Tangestaninejad, V. Mirkhani, I. Mohammadpoor-Baltork, *Appl. Catal. A* **2015**, *503*, 186–195.
- [92] X. Liu, N. Novoa, C. Manzur, D. Carrillo, J.-R. Hamon, *New J. Chem.* **2016**, *40*, 3308–3313.
- [93] A. Pourjavadi, M. Tajbakhsh, M. Farhang, S. H. Hosseini, *New J. Chem.* **2015**, *39*, 4591–4600.
- [94] Y. D. Bidal, M. Lesieur, M. Melaimi, F. Nahra, D. B. Cordes, K. S. A. Arachchige, A. M. Z. Slawin, G. Bertrand, C. S. J. Cazin, *Adv. Synth. Catal.* **2015**, *357*, 3155–3161.
- [95] E. A. Ison, A. Ison, *J. Chem. Educ.* **2012**, *89*, 1575–1577.
- [96] J. M. Barta, S. Díez-González, *Molecules* **2013**, *18*, 8919–8928.
- [97] M. K. Barman, A. K. Sinha, S. Nembenna, *Green Chem.* **2016**, *18*, 2534–2541.
- [98] D. P. Singh, B. K. Allam, K. N. Singh, V. P. Singh, *J. Mol. Catal. A* **2015**, *398*, 158–163.
- [99] N. Zohreh, M. Jahani, *J. Mol. Catal. A* **2017**, *426*, 117–129.
- [100] A. Salamatmanesh, M. K. Miraki, E. Yazdani, A. Heydari, *Catal. Lett.* **2018**, *148*, 3257–3268.
- [101] W. Kaim, J. Fiedler, *Chem. Soc. Rev.* **2009**, *38*, 3373–3382.
- [102] W. Kaim, A. Klein (Eds.), *Spectroelectrochemistry*, RSC Publishing, Cambridge, UK, **2008**.
- [103] COLLECT, Data Collection Software; Nonius B. V., Delft, Netherlands, **1998**.
- [104] Z. Otwinowski, W. Minor, in *Methods in Enzymology*, Vol. 276, Macromolecular Crystallography, Part A (Eds.: C. W. Carter, R. M. Sweet), Academic Press, London, Oxford, Boston, New York and San Diego **1997**, pp. 307–326.
- [105] SADABS 2016/2, see: L. Krause, R. Herbst-Irmer, G. M. Sheldrick, D. Stalke, *J. Appl. Crystallogr.* **2015**, *48*, 3–10.
- [106] G. M. Sheldrick, *Acta Crystallogr. Sect. A* **2015**, *71*, 3–8.
- [107] G. M. Sheldrick, *Acta Crystallogr. Sect. C* **2015**, *71*, 3–8.
- [108] A. L. Spek, *Acta Crystallogr. Sect. C* **2015**, *71*, 9–18.
- [109] XP, Siemens Analytical X-Ray Instruments Inc., Karlsruhe, Germany, **1990**; Madison, WI, USA, **1994**.

Manuscript received: December 15, 2020
Revised manuscript received: January 6, 2021
Accepted manuscript online: January 11, 2021